ISSN 1070-3284, Russian Journal of Coordination Chemistry, 2021, Vol. 47, No. 11, pp. 751–759. © Pleiades Publishing, Ltd., 2021.
Russian Text © The Author(s), 2021, published in Koordinatsionnaya Khimiya, 2021, Vol. 47, No. 11, pp. 689–697.

Complexes of Copper(II) Halides with 2-(3,5-Dimethylpyrazol-1-yl)benzimidazole: Synthesis and Magnetic and Cytotoxic Properties

A. D. Ivanova[a], T. A. Kuz'menko[b], A. I. Smolentsev[c], L. A. Sheludyakova[a], L. S. Klyushova[d], A. S. Bogomyakov[c, e], A. N. Lavrov[a], and L. G. Lavrenova[a, *]

[a] *Nikolaev Institute of Inorganic Chemistry, Siberian Branch, Russian Academy of Sciences, Novosibirsk, 630090 Russia*
[b] *Research Institute of Physical and Organic Chemistry, Southern Federal University, Rostov-on-Don, Russia*
[c] *Novosibirsk State University, Novosibirsk, 630090 Russia*
[d] *Institute of Molecular Biology and Biophysics, Federal Research Center of Fundamental and Translational Medicine, Novosibirsk, Russia*
[e] *International Tomography Center, Siberian Branch, Russian Academy of Sciences, Novosibirsk, Russia*
**e-mail: ludm@niic.nsc.ru*

Received March 17, 2021; revised May 12, 2021; accepted May 13, 2021

Abstract—New coordination compounds of copper(II) halides with 2-(3,5-dimethylpyrazol-1-yl)benzimidazole (L) are synthesized: $CuLCl_2$ (**I**), $[CuL_2Cl]Cl{\cdot}H_2O{\cdot}C_2H_5OH$ (**II**), and $CuLBr_2$ (**III**). The compounds are characterized by IR spectroscopy, X-ray diffraction analysis, and static magnetic susceptibility. The crystal structure of compound **II** is determined by X-ray structure analysis (CIF file CCDC no. 2043452). The cytotoxic properties of ligands L and complexes **I** and **II** are studied.

Keywords: synthesis, copper(II) complexes, 2-(3,5-dimethylpyrazol-1-yl)benzimidazole, X-ray structure analysis, X-ray diffraction analysis, IR spectroscopy, cytotoxic and magnetic activity

DOI: 10.1134/S1070328421110026

INTRODUCTION

2-(3,5-Dimethylpyrazol-1-yl)benzimidazole is of interest for synthesis and studies of the complexes having both nontrivial magnetic properties and biological activity. The benzimidazole derivatives possess a broad range of pharmacological properties. It is known that the complexation of biologically important organic compounds significantly increases their efficiency [1–4]. The complexes with the benzimidazole derivatives are characterized by anticancer activity and also act as antiviral and antimicrobial drugs [3, 5–9]. The copper(II) chloride complexes with the benzimidazole derivatives imitate the activity of superoxide dismutase (SOD), which is one of the main enzymes of the antioxidant system [10, 11]. Metalloenzymes (among which Cu,Zn-SOD is the most reactive) catalyze the dismutation of superoxide radical anions and decrease the probability of formation of more reactive singlet oxygen. In addition, SOD plays an important role in anti-aging mechanisms [12, 13].

We have previously synthesized and studied the coordination compounds of 4*H*-1,2,4-triazolo[1,5-a]benzimidazole and 2-methyl-, 3-methyl-, 4-methyl-, and 2,4-dimethyl-1,2,4-triazolo[1,5-a]benzimidazoles [14–16]. The copper(II) halide complexes with these ligands were shown to possess cytotoxic properties. In continuation of this work, it seemed reasonable to synthesize copper(II) halide complexes with 2-(3,5-dimethylpyrazol-1-yl)benzimidazole (L) and to study their magnetic and biological properties.

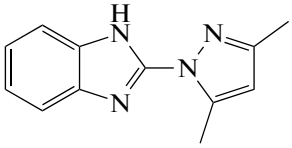

(L)

EXPERIMENTAL

Ethanol (rectificate), $CuCl_2{\cdot}2H_2O$, and $CuBr_2$ (both latter analytical grade) were used for the synthesis. All reagents were used as received. 2-(3,5-Dimethylpyrazol-1-yl)benzimidazole was synthesized using a procedure close to that described earlier [17, 18].

Synthesis of $CuLCl_2$ (I). Weighed samples of $CuCl_2{\cdot}2H_2O$ (0.18 g, 1 mmol) and L (0.21 g, 1 mmol) were dissolved separately in ethanol (5 mL) on heating, and the obtained solutions were mixed rapidly. The formed green solution darkened gradually. A brown precipitate was formed upon evaporation. The solution with the precipitate was evaporated to 1/2 of the initial volume and cooled in a crystallizer with ice.

The precipitate was filtered off on a Schott filter, washed two times with small portions (1–2 mL) of ethanol, and dried in air. The yield was 0.26 g (71%).

For $C_{12}H_{12}N_4Cl_2Cu$			
Anal. calcd., %	C, 41.6	H, 3.5	N, 16.2
Found, %	C, 41.6	H, 3.5	N, 16.0

Synthesis of $[CuL_2Cl]Cl{\cdot}H_2O{\cdot}C_2H_5OH$ (II). Weighed samples of $CuCl_2{\cdot}2H_2O$ (0.09 g, 0.5 mmol) and L (0.32 g, 1.5 mmol) were dissolved separately in ethanol (5 mL) on heating. A light green precipitate was formed on mixing the solutions. The precipitate was filtered off, washed, and dried similarly to that as described for the synthesis of compound **I**. The yield was 0.26 g (80%).

The crystals of compound **II** suitable for X-ray structure analysis (XSA) were formed on prolonged staying of the mother liquor.

For $C_{26}H_{32}N_8O_2Cl_2Cu$			
Anal. calcd., %	C, 50.1	H, 5.2	N, 18.0
Found, %	C, 50.1	H, 5.3	N, 17.9

Synthesis of $CuLBr_2$ (III). Weighed samples of $CuBr_2$ (0.22 g, 1 mmol) and L (0.21 g, 1 mmol) were dissolved separately in ethanol (5 mL) on heating. A brown precipitate was formed on mixing the solutions. The solution with the precipitate was evaporated in a water bath by 1/3 of the initial volume and then cooled in a crystallizer with ice. The precipitate was filtered off, washed, and dried in the same way as in the synthesis of compound **I**. The yield was 0.39 g (88%).

For $C_{12}H_{12}N_4Br_2Cu$			
Anal. calcd., %	C, 33.1	H, 2.8	N, 12.9
Found, %	C, 33.0	H, 3.0	N, 12.8

Elemental analyses of the complexes were carried out on a EUROEA 3000 instrument (EuroVector, Italy) at the analytical laboratory of the Nikolaev Institute of Inorganic Chemistry (Siberian Branch, Russian Academy of Sciences).

The X-ray diffraction analysis (XRD) of the polycrystalline samples was carried out on a Shimadzu XRD 7000 diffractometer (CuK_α radiation, Ni filter, scintillation detector) at room temperature. The samples were triturated in heptane and deposited on the polished side of a glass cuvette. Recording was carried out in an angle range of 5°–60° with an increment of 0.03° and exposure 1 s/point.

XSA was carried out using a standard procedure on Bruker-Noniusx8 APEX automated four-circle diffractometers for complex **II** (MoK_α radiation, λ = 0.71073 Å, graphite monochromator, two-coordinate 4K CCD detectors). An absorption correction was empirically applied by intensities of equivalent reflections (SADABS) [19]. The structure was solved by a direct method and refined by full-matrix least squares for F^2 in the anisotropic approximation for all non-hydrogen atoms using the SHELXS [20] and SHELXL [21] software and the OLEX2 graphical shell [22]. The high parameters of atomic shifts for solvate EtOH are related, most likely, to disordering over several close positions. The hydrogen atoms of ligand L were localized geometrically and refined by the riding model, the H atoms of the water molecules were localized from the difference Fourier synthesis and also refined by the riding model with the fixed values $U_{iso}(H) = 1.5U_{equiv}(O)$, and the H atoms of solvate EtOH were not localized from the difference synthesis and were revealed on the basis of geometric concepts. Selected crystallographic data and structure refinement details for compound **II** are presented in Table 1.

The coordinates of atoms and atomic shift parameters of the $[CuLCl_2]$ complex were deposited with the Cambridge Crystallographic Data Centre (CIF file CCDC no. 2043452; http://www.ccdc.cam.ac.uk/data_request/cif).

IR absorption spectra were recorded on Scimitar FTS 2000 and Vertex 80 spectrometers in a range of 4000–100 cm^{-1}. The samples were prepared as suspensions in Nujol, fluorinated oil, and polyethylene.

The magnetic properties of the polycrystalline samples were studied on an MPMS-XL SQUID magnetometer (Quantum Design) in the temperature range from 2 to 330 K and magnetic fields H = 0–10 kOe. To determine the paramagnetic component of the molar magnetic susceptibility ($\chi_p(T)$), the contributions of Larmor diamagnetism (χ_d) and ferromagnetism of microimpurities (χ_F) were subtracted from the measured values of the total molar susceptibility $\chi = M/H$ (M is magnetization): $\chi_p(T,H) = \chi(T,H) - \chi_d - \chi_F(T,H)$. The temperature-independent contribution χ_d was calculated according to Pascal's additive scheme, and the field dependences $M(H)$ and dependences $M(T)$ at various magnetic field strengths were measured to determine the ferromagnetic contribution χ_F. In the studied samples, $\chi_F < \chi_d$ at $H > 2$ kOe. The effective magnetic moment was calculated by the equation $\mu_{eff} = [3k\chi_pT/(N_A\mu_B^2)]^{1/2} \approx (8\chi_pT)^{1/2}$, where N_A, μ_B, and k are Avogadro's number, Bohr magneton, and Boltzmann constant, respectively.

The cytotoxic effect of the ligands and complexes were studied on the Hep-2 cell line (human laryngeal carcinoma) kindly presented by the colleagues from the State Research Center of Virology and Biotechnology Vector. The cells were seeded on 96-well plates (5×10^3 cells per well) and cultivated in Dulbecco's Minimum Essential Medium (DMEM) with the 10% content of fetal bovine serum (FBS, HyClone) in a wet atmosphere containing 5% CO_2 at 37°C. In 24 h,

Table 1. Crystallographic characteristics, experimental XRD details, and structure refinement results for compound **II**

Parameter	Value
Empirical formula	$C_{26}H_{32}N_8O_2Cl_2Cu$
FW	623.03
Crystal system	Triclinic
Space group	$P\bar{1}$
a, Å	10.6268(2)
b, Å	13.0137(3)
c, Å	13.0520(3)
α, deg	103.0220(10)
β, deg	113.3540(10)
γ, deg	108.9560(10)
V, Å^3	1431.01(6)
Z	2
ρ_{calc}, g cm^{-3}	1.446
$\mu(MoK_\alpha)$, mm^{-1}	0.989
Crystal size, mm	0.4 × 0.3 × 0.2
Range of data collection over θ, deg	1.81 – 27.53
Ranges of *h*, *k*, *l*	$-13 \le h \le 13$, $-15 \le k \le 16$, $-16 \le l \le 16$
Number of measured reflections	14929
Number of independent reflections (R_{int})	6520 (0.0213)
Number of refined parameters	451
F(000)	646
$R\,(F^2 > 2\sigma(F^2))$	$R_1 = 0.0383$, $wR_2 = 0.1107$
$R\,(F^2)$	$R_1 = 0.0445$, $wR_2 = 0.1164$
GOOF	1.033
$\Delta\rho_{max}/\Delta\rho_{min}$, e Å^{-3}	0.84/–0.61

the studied compounds dissolved in ethanol or in a 50% water–ethanol solution were added in a concentration range of 0.2–125 μM, and the resulting solutions were incubated for 48 h. The final concentration of the solvent in the medium did not exceed 1%. Then the cells were stained with the Hoechst 33342 (at 37°C within 30 min) and Propidium Iodide (at 37°C within 10 min) fluorescent dyes [23]. After the indicated time passed, the medium in the well was changed to remove a dye excess. Recording was performed on an IN Cell Analyzer 2200 (GE) instrument in the automatic mode using 4 fields per well. The obtained images were examined using the IN Cell Investigator software (GE Healthcare, UK) for the determination of the percentage content of each group of cells (normal, apoptosis, and dead) in the whole population due to the action of the studied compounds. The result was presented as a percentage ratio of the cells from three independent experiments ± standard deviation. The half-maximal inhibitory concentration (IC_{50}) determined as the concentration of the compound at which the cell decay was 50% was calculated after the approximation of the curves of the experimental dependence of cell survival (%) on the concentration of the studied compound (μM) by the nonlinear function.

RESULTS AND DISCUSSION

Complexes **I**–**III** were isolated from water–ethanol solutions at different metal to ligand ratios. The ratios were experimentally selected to obtain the phase

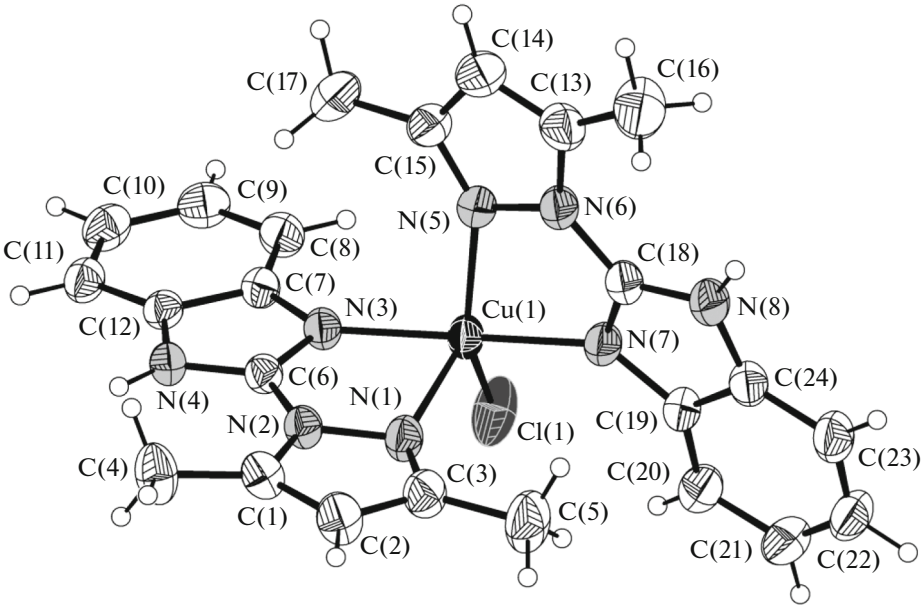

Fig. 1. Structure of the $[CuL_2Cl]^+$ complex cation in compound **II**. Atomic shift ellipsoids of 50% probability are presented.

of a certain composition. According to the XRD data, all compounds are crystalline, but there are no isostructural compounds among them.

The XSA data show that complex $[CuL_2Cl]Cl\cdot H_2O\cdot C_2H_5OH$ (**II**) crystallizes in the triclinic crystal system, space group $P\bar{1}$, $Z = 2$ (Table 1). The independent part of the unit cell contains the complex cation $[CuL_2Cl]^+$, outer-sphere chloride anion, one crystallization water molecule, and one crystallization ethanol molecule. The cation is noncentrosymmetric, and the coordination environment of the central Cu^{2+} ion is a distorted tetragonal pyramid formed by four nitrogen atoms of two ligands L coordinated via the bidentate mode and one chloride anion (Fig. 1). The Cu–N bond lengths range from 1.9761(18) to 2.2650(18) Å, and the highest value is observed for the N(1) atom located at the vertex of the coordination pyramid.

The τ descriptor can be used for the quantitative description of the five-membered coordination mode that takes place in complex **II**: $\tau = (\alpha - \beta)/60$ as proposed earlier [24] (α and β are two largest LML angles, $\alpha > \beta$). Evidently, parameter τ in the range from 0 to 1 determines any combination of states of a tetragonal pyramid and a trigonal bipyramid in the geometry of the coordination polyhedron. In complex **II**, two largest angles NCuN and NCuCl are 169.32(8)° and 145.96(6)°, respectively. Thus, the τ descriptor equal to 0.389 allows the quantitative characterization of the coordination polyhedron $[CuN_4Cl]$ as close to a tetragonal pyramid with a sufficiently high (38.9%) contribution of the trigonal bipyramid state.

The main bond angles are given in Table 2. Strong hydrogen bonds of four types are observed: N–H···O between ligands L and water molecules (distance N···O 2.732(2) Å), N–H···Cl between ligands L and chloride anions (distance N···Cl 3.112(2) Å), O–H···Cl between water molecules and chloride anions (both outer- and inner-sphere; distances O···Cl 3.103(2) and 3.155(2) Å), and O–H···Cl between ethanol molecules and outer-sphere chloride anions (distance O···Cl 3.302(6) Å). These hydrogen bonds lead to the formation of chains parallel to the [–1 1 0] direction in which all structural units are involved (Fig. 2). Ligands L within the chain are oriented pairwise parallel to the minimum interplanar distance equal to ~3.3 Å, thus indicating the presence of π–π interactions.

The IR spectrum of L in a high-frequency range of 3300–2500 cm^{-1} exhibits a broad medium-intensity absorption band of the NH groups involved in the formation of hydrogen bonds. Weakly pronounced maxima of the bands ν(CH) of the ring and $\nu(CH_3)$ are observed in a range of 3100–2800 cm^{-1}. The spectra of complexes **I**–**III** are similar. The ν(NH) and ν(CH) bands in them become more distinct than those in the spectrum of L, which is probably related to a change in the character of hydrogen bonds during complex formation.

The number and position of the bands in a range of 1620–1480 cm^{-1} (ring vibrations, R) change substantially compared to the spectrum of L (Table 3). This suggests (on the basis of the XSA data for complex **II**) the coordination of the nitrogen atoms of the cycles to the Cu^{2+} ion in all synthesized complexes. The bands

Table 2. Selected geometric characteristics of the $[CuL_2Cl]^+$ cation in the structure of compound **II**

Bond	*d*, Å	Bond	*d*, Å
Cu(1)–N(1)	2.2650(18)	Cu(1)–N(7)	1.9761(18)
Cu(1)–N(3)	1.9800(17)	Cu(1)–Cl(1)	2.2598(7)
Cu(1)–N(5)	2.0872(18)		
Angle	ω, deg	Angle	ω, deg
N(1)Cu(1)N(3)	76.39(7)	N(5)Cu(1)N(7)	78.74(7)
N(1)Cu(1)N(5)	100.27(7)	N(1)Cu(1)Cl(1)	113.72(5)
N(1)Cu(1)N(7)	95.60(7)	N(3)Cu(1)Cl(1)	94.14(5)
N(3)Cu(1)N(5)	95.56(7)	N(5)Cu(1)Cl(1)	145.96(6)
N(3)Cu(1)N(7)	169.32(8)	N(7)Cu(1)Cl(1)	95.58(6)

that are absent in the spectrum of L appear in the low-frequency range (400–200 cm^{-1}) and were assigned to ν(Cu–N) and ν(Cu–Hal).

Thus, the data of elemental analysis and IR spectroscopy indicate that the coordination mode in complexes **I** and **III** occurs due to the nitrogen atoms of L coordinated via the bidentate-cyclic mode and two halide ions located in the internal sphere. The internal sphere of complex **II** contains two L molecules and one chloride ion, and the external sphere contains the second chloride ion and the water and ethanol molecules. The character of the IR spectra agrees with the XSA data for complex **II**.

The temperature dependences of μ_{eff} and inverse magnetic susceptibility ($1/\chi_p$) for complexes **I** and **II** are presented in Fig. 3. For complex **I**, $\mu_{eff} = 1.85\ \mu_B$ at 300 K and remains nearly unchanged with temperature decreasing to 50 K. After this, μ_{eff} decreases reaching 1.38 μ_B at 5 K. For complex **II**, $\mu_{eff} = 1.80\ \mu_B$ at 300 K and remains unchanged on cooling to the helium temperatures. The $1/\chi_p(T)$ dependences for complexes **I** and **II** are linear and satisfactorily described by the Curie–Weiss law with the optimum values of parameters C and θ equal to 0.433 K cm^3 mol^{-1} and –2.8 K for complex **I** and 0.408 K cm^3 mol^{-1} and –0.7 K for complex **II**. The values of μ_{eff} at 300 K and Curie constants C for complexes **I** and **II** are well consistent with theoretical spin-only values of 1.86 μ_B and 0.433 K cm^3 mol^{-1} for one copper(II) ion with the spin $S = 1/2$ at $g = 2.15$. A decrease in μ_{eff} at temperatures lower than 50 K and the value of the Weiss constant θ for complex **I** indicate weak antiferromagnetic exchange interactions. There are no significant exchange interactions for complex **II**, which is indicated by the constant value of μ_{eff} in a wide temperature range and a low Weiss constant (θ).

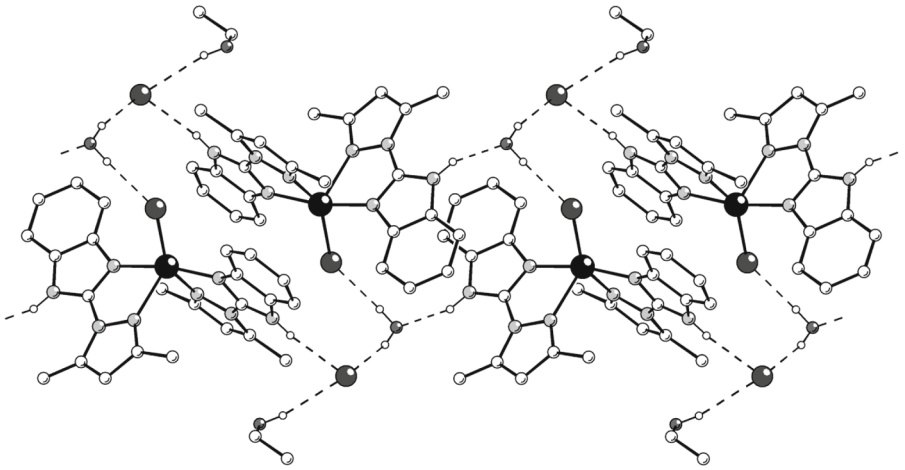

Fig. 2. Fragment of the chain formed due to hydrogen bonds (dashed lines) between the $[CuL_2Cl]^+$ complex cations, Cl^- ions, and water and ethanol molecules. Only the hydrogen atoms involved in hydrogen bond formation are shown.

Table 3. Vibrational frequencies (cm^{-1}) in the IR spectra of the ligand and complexes in the range of vibrations of the ring *R* and in the low-frequency range

Compound				Assignment
L	**I**	**II**	**III**	
1626 1593 1572 1558 1482	1579 1512 1480	1614 1576 1567 1504	1579 1511 1481	R_{ring}
	292 276	253	274	ν(Cu–N)
	315	318		ν(Cu–Cl)
			246	ν(Cu–Br)

The magnetic properties of the $CuLBr_2$ complex (**III**) differ substantially from those of the complexes containing chloride ions. Although in a temperature range of 50–330 K the temperature dependence of the susceptibility $\chi_p(T)$ for both complexes **I** and **II** is well described by the Curie–Weiss law with the close values of μ_{eff}, the $\chi_p(T)$ dependence substantially deviates from the paramagnetic behavior with temperature decreasing and passes through a maximum at $T_m \approx 20$ K (Fig. 4). A decrease in the susceptibility at low temperatures and a high negative value of the Weiss constant $\theta \approx -25$ K indicate substantially stronger antiferromagnetic exchange interactions in this complex. A broad and flat maximum in the $\chi_p(T)$ dependence is a characteristic property of low-dimensional magnetics and points to the formation of magnetic chains of Cu^{2+} ions with strong intrachain and weak interchain exchange interactions. The intrachain antiferromagnetic exchange interaction *J* can qualitatively be evaluated from the values of T_m and θ at the level of $J/k_B \approx 20$ K. Note that spin correlations in the chains begin to develop already from the temperatures ~50 K, which is observed as a significant decrease in μ_{eff} (Fig. 4).

The influence of ligand L and its copper(II) chloride and bromide complexes on the Hep-2 cell line was studied. The morphological changes in the Hep-2 cells are shown in Fig. 5. The values of IC_{50} are given in Table 4. Ligand L exerted no cytotoxic effect on this cell line in the studied concentration range (0.2–125 μM). The data obtained show that complex **I** is the most toxic, since its effect resulted in cell decay at a level of 50% (1 μM) among which the percentage of the cells exhibiting the morphological changes in the nuclei (characteristic of apoptosis) was 30% (Fig. 6). The cytotoxicities of complexes **II** and **III** are comparable. The values of IC_{50} are 3.6 ± 0.3 (**II**) and 3.1 ± 0.3 (**III**) μM.

In [19–21] we studied the cytotoxicity of a series of the complexes with triazolo[1,5-a]benzimidazoles differed from L by one additional condensed heterocycle. Note that the copper(II) compounds with 2-(3,5-dimethylpyrazol-1-yl)benzimidazole studied in this work are characterized by a substantially higher cytotoxicity than that of the previously synthesized complexes (Table 4).

Thus, the new compounds of copper(II) halides with 2-(3,5-dimethylpyrazol-1-yl)benzimidazole (L)

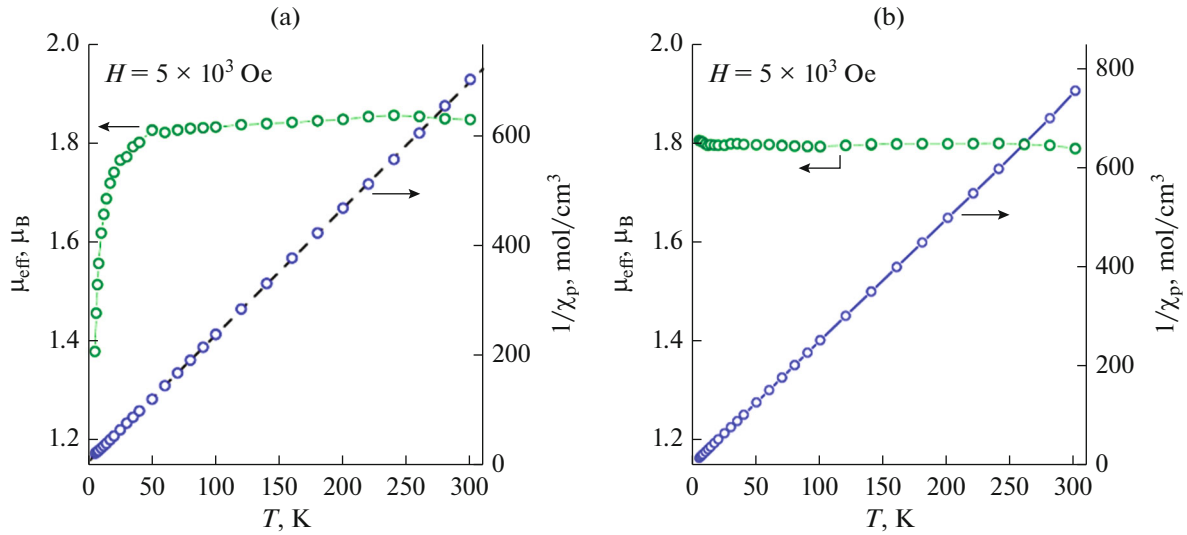

Fig. 3. Temperature dependences of μ_{eff} and $1/\chi_p$ for (a) complex $CuLCl_2$ and (b) $[CuL_2Cl]Cl \cdot H_2O \cdot EtOH$. Dashed line on panel (a) indicates the result of data processing according to the Curie–Weiss dependence.

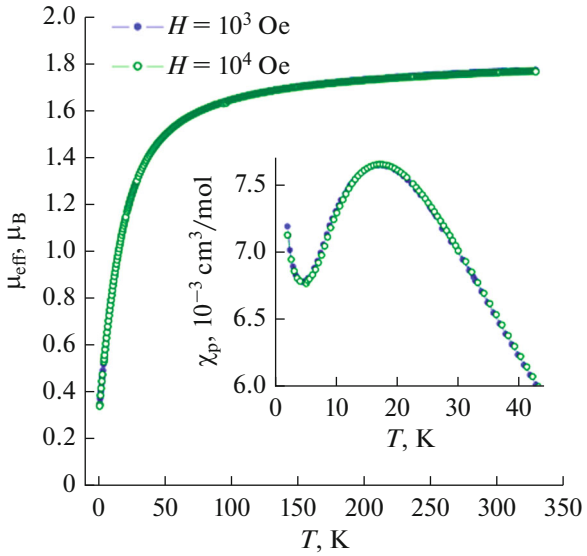

Fig. 4. Temperature dependence of μ_{eff} for complex $CuLBr_2$ measured in the magnetic field H = 1 kOe (●) and 10 kOe (○). Inset: the temperature dependences of χ_p in the low-temperature range.

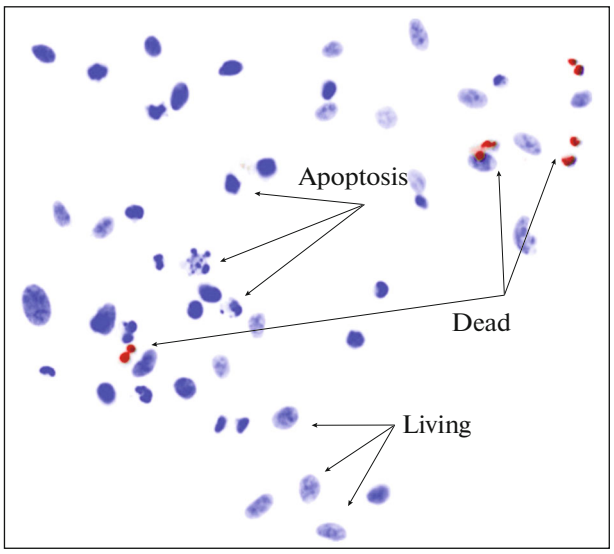

Fig. 5. Representative image showing the morphological changes of the Hep-2 cells after incubation with 1 μM $CuLCl_2$ (**I**) found using the Hoechst 33342/PI double staining protocol.

Table 4. Values of IC_{50} for complexes **I**–**III**, the previously studied complexes [14–16], and cisplatin

Compound	IC_{50}, μM	Literature
$CuLCl_2$ (**I**)	1.1 ± 0.1	This work
$[CuL_2Cl]Cl$ (**II**)	3.6 ± 0.3	This work
$CuLBr_2$ (**III**)	3.1 ± 0.3	This work
$Cu(L^1)_2Cl_2$*	65.4	[14]
$Cu(L^2)_2Cl_2$*	65.9	[14]
$[Cu_2(L^3)_4(\mu\text{-}Br)_2Br_2]$**	17.0	[15]
$Cu(L^4)_2Cl_2$***	98.0	[16]
Cisplatin	9.2 ± 0.5	[25]

* L^1 is 4*H*-1,2,4-triazolo[1,5-a]benzimidazole, L^2 is 4-methyl-1,2,4-triazolo[1,5-a]benzimidazole.
** L^3 is 2-methyl-1,2,4-triazolo[1,5-a]benzimidazole.
*** L^4 is 2,4-dimethyl-1,2,4-triazolo[1,5-a]benzimidazole.

were synthesized: $[CuLCl_2]$, $[CuL_2Cl]Cl{\cdot}H_2O{\cdot}C_2H_5OH$, and $[CuLBr_2]$. The cytotoxic properties of ligand L and the synthesized complexes were studied on the Hep-2 cell line. The obtained data show that the $CuLCl_2$ complex is the most toxic and its action leads to the cell decay at a level of 50% (1 μM). The percentage of the cells manifested morphological changes in the cell nucleus characteristic of apoptosis was 30%. A comparison of the obtained results with the literature data shows that the cytotoxicity of $CuLCl_2$ is comparable with that for cisplatin. The value of IC_{50} is (1.1 ± 0.1) μM [25].

ACKNOWLEDGMENTS

The authors are grateful to N.P. Korotkevich for obtaining XRD patterns and to I.V. Yushin for recording diffuse reflectance spectra.

Experiments on cytotoxicity tests were carried out on the basis of the Center for Collective Use "Proteomic Anal-

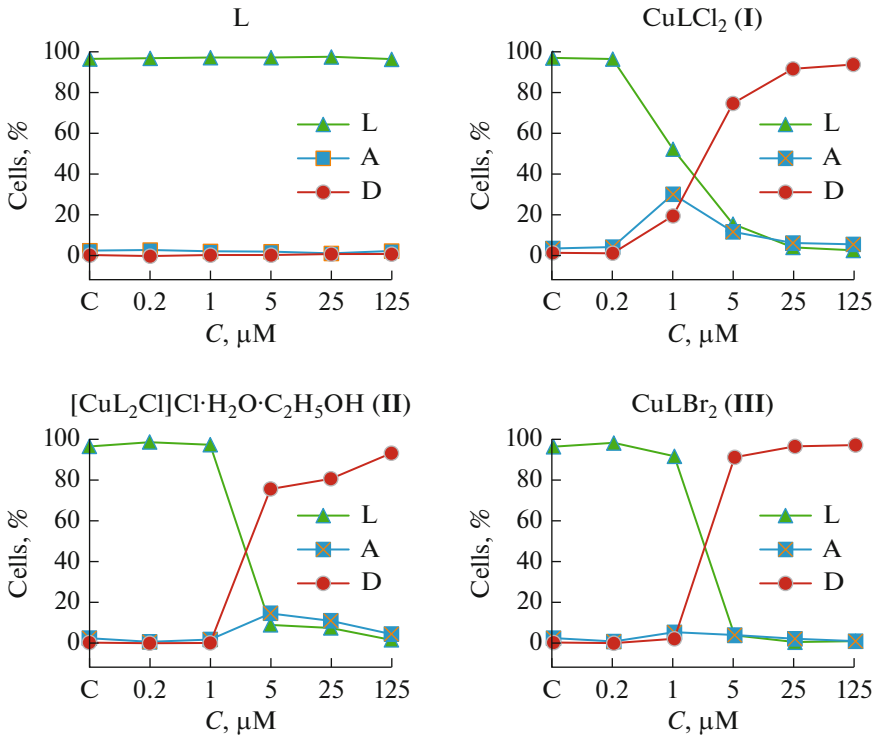

Fig. 6. Results of the treatment of the Hep-2 cells with solutions of the compounds for 48 h: (▲) living cells, (■) apoptosis cells, and (●) dead cells.

ysis" of the Institute of Molecular Biology and Biophysics (Federal Research Center of Fundamental and Translational Medicine, Novosibirsk, Russia).

FUNDING

This work was supported by the Russian Science Foundation (project no. 20-63-46026) and the Ministry of Science and Higher Education of the Russian Federation (projects nos. 121031700313-8, and 121031700314-5, and FENW-2020-0031 (0852-2020-0031) (state assignment of the Southern Federal University)).

CONFLICT OF INTEREST

The authors declare that they have no conflicts of interest.

REFERENCES

1. Yurdakul, S. and Kurt, M., *J. Mol. Struct.*, 2003, vol. 650, p. 181.
2. Singh, V.P., Katiyar, A., and Singh, S., *J. Coord. Chem.*, 2009, vol. 62, p. 1336.
3. Gumus, F., Algul, O., Eren, G., et al., *Eur. J. Med. Chem.*, 2003, vol. 38, p. 473.
4. Sau, D.K., Butcher, R.J., Chaudhuri, S., and Saha, N., *Mol. Cell. Biochem.*, 2003, vol. 253, p. 21.
5. Spasov, A.A., Yozhitsa, I.N., Bugaeva, L.I., and Anisimova, V.A., *Pharm. Chem. J.*, 1999, vol. 33, p. 232.
6. Gocke, M., Utku, S., Gur, S., et al., *Eur. J. Med. Chem.,* 2005, vol. 40, p. 135.
7. Bharti, N., Shailendra, M.T., Garza, M.T.G., et al., *Bioorg. Med. Chem. Lett.*, 2002, vol. 12, p. 869.
8. Mothilal, K.K., Karunakaran, C., Rajendran, A., and Murugesan, R., *J. Inorg. Biochem.*, 2004, vol. 98, p. 322.
9. Podunavac-Kuzmanovic, S.O. and Cvetcovic, D.M., *J. Serb. Chem. Soc.*, 2007, vol. 72, p. 459.
10. Sączewski, F., Dziemidowicz-Borys, E.J., Bednarski, P.J., et al., *J. Inorg. Biochem.*, 2006, vol. 100, p. 1389.
11. Volykhina, V.E. and Shafranovskaya, E.V., *Vest. Vitebsk. Gos. Med. Univ.*, 2009, vol. 8, no. 4, p. 1.
12. Farmer, K.J. and Sohal, R.S., *Free Radicals Biol. Med.*, 1989, vol. 7, p. 23.
13. Rusting, R.L., *Sci. Am.*, 1992, vol. 267, p. 88.
14. Lavrenova, L.G., Kuz'menko, T.A., Ivanova, A.D., et al., *New J. Chem.*, 2017, vol. 41, p. 4341.
15. Dyukova, I.I., Kuz'menko, T.A., Komarov, V.Y., et al., *Russ. J. Coord. Chem.,* 2018, vol. 44, p. 755. https://doi.org/10.1134/S107032841812014X
16. Dyukova, I.I. Lavrenova, L.G., Kuz'menko, T.A., et al., *Inorg. Chim. Acta*, 2019, vol. 486, p. 406.
17. Klyuyev, N.A., Povstyanoi, M.V., Aleksandrov, G.G., and Gumennyi, V.P., *Khim. Geterotsikl. Soed.*, 1983, no. 1, p. 88.
18. Hawes, C. and Kruger, P., *Supramol. Chem.*, 2015, vol. 27, nos. 11–12, p. 757.

19. *APEX2 (version1.08), SAINT (version 7.03), SADABS (version 2.11), SHELXTL (version 6.12)*, Madison: Bruker AXS Inc., 2004.
20. Sheldrick, G.M., *Acta Crystallogr., Sect. A: Found. Crystallogr.*, 2008, vol. 64, p. 112.
21. Sheldrick, G.M., *Acta Crystallogr., Sect. C: Struct. Chem.*, 2015, vol. 71, p. 3.
22. Dolomanov, O.V., Bourhis, L.J., Gildea, R.J., et al., *J. Appl. Crystallogr.*, 2009, vol. 42, p. 339.
23. Lee, Y.-J. and Shacter, E., *Blood*, 1997, vol. 89, p. 4480.
24. Addison, A.W., Rao, T.N., Reedijk, J., et al., *Dalton Trans.*, 1984, vol. 7, p. 1349.
25. Makhinya, A.N., Eremina, J.A., Sukhikh, T.S., et al., *ChemistrySelect.*, 2019, vol. 4, p. 5866.

Translated by E. Yablonskaya